The role of benthic biofilm production in the mediation of silicon cycling in the Severn Estuary, UK

Welsby, H.J.[1,2], Hendry, K.R.[2], Perkins, R.G.[1]

[1]School of Earth and Ocean Science, Main Building, Cardiff University, Cardiff, CF10 3AT, UK.

[2]School of Earth Sciences, University of Bristol, Wills Memorial Building, Queens Road, Bristol, BS8 1RJ, UK.

Abstract

1   The biological mediation of benthic biogenic silica (BBSi) by the diatom-dominated
2   biofilms on the intertidal mudflats of the Severn Estuary (UK) was assessed *in situ*
3   under different environmental conditions using measurements of productive biomass
4   (chlorophyll *a*), photosynthetic activity of undisturbed microalgal assemblages, benthic
5   biogenic silica (BBSi) and benthic dissolved silica (BDSi). We show low BBSi standing
6   stocks in the mudflats compared to other European estuaries, under both warmer
7   summer conditions (0.6%) and colder winter conditions (0.5%). Dissolved forms of Si
8   (BDSi) dominated the estuary, with significantly higher concentrations during the
9   sampled winter (22.6 ± 1.0 mg L^{-1}) compared to the sampled summer (2.9 ± 0.5 mg L^{-1}
10   ). Benthic algal biomass was higher under cold conditions compared to warmer
11   conditions (24.0 ± 2.3 and 13.2 ± 1.9 mg g^{-1} *sed. dw.*, respectively), following reduced
12   migratory behaviour in the winter increasing surficial biomass. Relative maximum
13   Electron Transport Rate (rETR$_{max}$), used as a proxy for relative primary productivity,
14   was higher under warm conditions (254.1 ± 20.1 rel. units) compared to cold conditions
15   (116.0 ± 27.1 rel. units). The biofilms sampled in the summer biologically mediated Si
16   by the productive, high light acclimated diatoms that were highly motile during
17   fluorescence measurements, and exhibited migratory behaviour, which despite
18   nutrient limitation, evidenced by low F_v/F_m, increased the accumulation of BBSi. The
19   biofilms sampled in the winter that were subject to relatively colder temperatures,
20   consisted of low light acclimated diatoms of reduced migratory capabilities, and
21   induced NPQ that suppressed productivity, and mediated BBSi to a lesser extent.
22   Environmental stresses reduced biofilm mediation of Si, which, in addition to high

23 hydrodynamic energy increasing biofilm re-suspension, controlled Si to a lesser extent
24 compared to terrestrial/coastal inputs.

Keywords

26 Biogenic silica, benthic, biomass, primary productivity, downregulation.

Introduction

28 Most research on the global silicon (Si) cycle has focused on weathering (Hurd, 1977;
29 West et al. 2005; Fortner et al. 2012) or oceanic Si cycles (Brzezinski et al. 1998; Yool
30 & Tyrrell, 2003). Few have explored the complexity of the marine-terrestrial
31 interconnecting cycles, leaving estuarine processes poorly constrained despite their
32 importance in determining marine Si budgets. The present study intends to address
33 the lack of research on Si cycling in the coastal transition zone. This was achieved by
34 analysing the variations in Si fractions in the Severn Estuary, resulting from
35 environmental driven changes in the ecosystem functioning, in the form of biomass
36 and relative primary productivity, by the exposed diatom-dominated (Underwood,
37 2010) microphytobenthos (MPB) biofilms on the intertidal mudflats.

38 The high water turbidity, typical of a sediment-dominated estuary, limits the growth of
39 large pelagic phytoplankton communities (Underwood, 2010). Subsequently, the MPB
40 biofilms have high rates of biogeochemical cycling, with complex rhythms of
41 photosynthetic activity (Pickney & Zingmark, 1991), and are likely to mediate nutrient
42 dynamics in an estuary. MPB are characterized by the absence of photo-inhibition at
43 high irradiance, due to the combination of physiological (e.g. effective photochemical
44 and non-photochemical quenching, NPQ; *see* Maxwell & Johnson, 2000; Jesus et al.
45 2006; Lavaud & Kroth, 2006) and behavioural mechanisms (bulk migratory response),
46 and cell surface turnover in the form of micro-cycling, minimizing the risk of
47 overexposure to damaging light intensities (Kromkamp et al. 1998; Serôdio et al.
48 2006b, 2008; Perkins et al. 2001, 2002, 2010). No previously published studies have
49 investigated the diatom-dominated MPB biofilms influence on Si dynamics in the
50 Severn Estuary.

51 The Severn Estuary is a heterogeneous environment with a complex hydro-
52 geomorphology (Kirby, 2010; Manning et al. 2010), resulting in an important
53 environment for biosphere functioning, primarily through the filter for land-ocean
54 exchange. The hyper-tidal range is the second highest astronomical tide globally (13.9

m at Avonmouth) (Liang et al. 2013) resulting in substantial intertidal areas of cohesive muddy sediment. This makes the Severn Estuary an important case study for Si cycling, and allows for scaling to quantify other estuarine Si budgets. Few estuarine Si studies exist globally (De'Elia et al. 1983; Rendell et al. 1997; Liu et al. 2005; 2008; 2009; Arndt & Regnier, 2007; Pastuszak et al 2008; Carbonnel et al. 2009; 2013), and understanding of the controls on the current Si cycle and estuarine budgets are lacking. The Scheldt Estuary, Belgium/The Netherlands, remains one of the only estuaries to have a comprehensive Si dataset, and has proven to enhance biological processes leading to nutrient transformations (Arndt & Regnier, 2007; Carbonnel et al. 2009; 2013). Similarly, the fine-sediment dominated Severn Estuary may exhibit a significant biological control on Si dynamics. Further, the strength of the inter-habitat coupling in the estuary implies that changes in MPB biomass and productivity may propagate into other linked ecosystems, and further afield to the marine pelagic zone in the southwest.

Si is a key element for siliceous organisms in aquatic habitats. Land-sea interactions and transfers control the proportions of Si in the form of silicic acid $Si(OH)_4$, hereafter called 'dissolved silica' (DSi), and particulate biogenic silica (BSi). These vary seasonally and geographically due to the transformation from DSi to BSi (~240 t mol y^{-1}) by photoautotrophic motile epipelic diatoms (accounting for >95% of eukaryotic living cells on intertidal mudflats) (Underwood, 2010), and weathering processes, a factor of river flow regime and temperature (Ragueneau et al. 2000). The variation in the natural abundance of Si fractions has often been used as a proxy for diatom production and Si utilization (Conley & Malone, 1992). Therefore, characterizing the difference in Si fractions provides important information on Si biological uptake in the estuary.

Si cycling is poorly quantified from local to global scales due to the lack of Si data compared to other key nutrients (Moosdorf et al. 2011). Previous studies (Conley & Malone, 1992; Aure et al. 1998; Gilpin et al. 2004) have noted non-Redfield ratios (Redfield et al. 1963) in estuaries. For example, in sub areas of the Baltic Sea, the doubling of phosphate and nitrate inputs increased BSi production causing a reduction in DSi, and induced Si limitation (Pastuszak et al. 2008). Such nutrient ratios can diminish the relative importance of diatoms, resulting in non-siliceous phytoplankton becoming dominant (Correll et al. 2000). Despite the Severn Estuary's ecological and economic importance, its role in benthic BSi (BBSi) and benthic DSi (BDSi) transformations, to our knowledge, has not been addressed quantitatively. This gap

90　leaves little understanding of the terrestrial disturbances by anthropogenic activities,
91　land-use changes, and climate change expected over the twenty-first century (Met
92　Office, 2011). The aim of this study was to analyse the biological mediation of Si by
93　the diatom-dominated MPB biofilms in the Severn Estuary under different
94　environmental conditions, resulting from investigating three separate survey sites
95　under summer and winter conditions. This was achieved through the analysis of
96　different environmental conditions experienced during the summer (relatively warmer,
97　lower rainfall) and a winter (relatively colder, higher rainfall), and over a spatial scale
98　of the three sample sites that differed in sediment water content and site exposure.

99　## Methods

100　**Study site and sampling method**

101　The study was carried out on intertidal mudflats located in the Severn Estuary between
102　southeast Wales and southwest England (Fig. 1). Three intertidal mudflat sites were
103　surveyed: site 1, Severn Beach (002°66'W, 051°56'N); site 2, Portishead (002°77'W,
104　051°49'N); and site 3, Newport Wetlands (002 °58'W, 051°32'N). Site 1 mudflats
105　located at the mouth of the River Severn, subject to a small tidal prism, were exposed
106　to the full-force of the prevailing south westerly winds, and had sediments of high sand
107　content (>63 μm). Site 2 mudflats were less exposed to the south westerly winds, and
108　had higher mud content (<63 μm), and crevasses perpendicular to the shoreline. Site
109　3 mudflats, subject to a large tidal prism, were sheltered from the south westerly winds,
110　and had high mud content (<63 μm), and laid adjacent to a saltmarsh and wetlands.

111　*In situ* MPB biofilms were sampled during daytime low tide periods in the summer and
112　winter of 2014. Air temperature records for the Severn Estuary show a significant
113　difference (t(df)=13.224, $p<0.001$) between the relatively warmer summer and
114　relatively colder winter sampling periods (Fig. 2) (Met Office, 2015). The benthic
115　biofilms sampled during the summer were exposed to longer sunshine hours and lower
116　rainfall (225 hrs sunshine, 79.6 ± 28.2 mm of rain) compared to biofilms sampled during
117　the winter (64 hrs sunshine and 136.8 ± 28.6 mm of rain) (Met Office, 2015).

118　At each site, 12 sampling stations were surveyed, equally spaced along a linear
119　transect parallel to the lower shore. Sampling involved extracting sediment mini-cores
120　of a diameter of 2.54 cm for the surficial 5 mm biofilm for analyses of chlorophyll *a*
121　content (chl *a*) (Smith & Underwood, 1998), key benthic diatom species, and BBSi

122 content. Pore fluids (25 ml) at each station were sampled for BDSi and orthophosphate

123 (P) concentrations using a simplified peeper method (Teasdale et al. 1995).

BBSi

125 Approximately 25% of the surficial 5 mm biofilm sediment was placed in an oven at

126 85°C for 24 h to determine the percentage loss of weight upon drying. BBSi

127 concentrations were determined following the standard alkaline extraction method for

128 marine sediment (DeMaster, 1981) and presented as percentage of dried Si mass

129 (g/g). Dried sediment was crushed using a pestle and mortar, and ~0.05 g of the

130 sediment was leached in hydrogen peroxide (5 ml of 10% H_2O_2 solution), followed by

131 acid (5 ml of 1M HCl solution). To each sample, 40 ml of 0.1 M of $NaCO_3$ was added.

132 Samples were placed in a covered, constant temperature water bath at 85°C. After 1

133 h, 3 h and 5 h, sub samples were taken, diluted, neutralized, and analysed for BBSi

134 content using the standard Heteropoly Blue Method, and measured using a Hach

135 Lange DR3900 spectrophotometer.

BDSi and orthophosphate (P-PO$_4^-$)

137 Pore fluid samples were centrifuged for 10 min at 1000 rpm for BDSi and P-PO$_4^-$

138 concentrations. BDSi was analysed using the Heteropoly Blue method with

139 concentrations (mg L^{-1}) measured using a Hach Lange DR3900 spectrophotometer.

140 P-PO$_4^-$ concentrations (mg L^{-1}) from pore fluids were measured using a Hach Lange

141 DR3900 spectrophotometer, where 2.0 ml of each sample were analysed following the

142 LCK 349 method. All P-PO$_4^-$ concentrations recorded in both seasons, were below 50

143 mg L^{-1} and did not interfere with BBSi measurements.

MPB biofilm biomass and key species

145 Half of the surficial 5 mm of the sediment from the mini-cores was extracted, weighed

146 (g) and corrected for water content (loss of weight upon drying at 85°C for 24 h) (*see*

147 Perkins et al. 2003). Productive biomass via chl *a* content (mg g^{-1} *sed. dw.*) were

148 determined following the standard method (extraction in methanol; Shwartz & Lorenzo,

149 1990), with 4 ml of methanol buffered with $MgCO_3$ added to each sediment sample

150 and left at -4°C and in the dark for 24 h. Samples were vortex mixed and centrifuged

151 at 2000 rpm for 15 min. Chl *a* values were corrected for phaeopigments through

152 acidification following the standard method (Lorenzen, 1966), with absorbance

153 measured at 665 nm and 750 nm and repeated following the addition of 1 drop of 10%

154 HCl to each plastic micro-cuvette.

155 Species composition of the biofilms were determined by filtering approximately 25% of

156 the surficial 5 mm sediments with DI water to remove silts and fine sediment grains.
157 Due to the low biomass, the suspended fractions were placed in petri dishes and
158 diatoms were viewed using bright-field microscopy for the determination of key diatoms
159 species. Individual diatoms were mounted, dried and gold plated for imaging using the
160 Environmental Scanning Electron Microscope (FEI XL30 ESEM FEG).

Chlorophyll fluorescence

162 Variable chlorophyll fluorescence of undisturbed microalgae assemblages was
163 determined using a Water Pulse Amplitude Modulated (PAM) fluorometer equipped
164 with an EDF/B fibre optic detector (blue light measuring beam and actinic light). The
165 Water PAM 6 mm diameter Fluid Light Guide fiberoptics probe bundle (that delivered
166 the measuring and saturating light provided by the fluorometer) was applied to the
167 surface of the mudflat perpendicularly, at a fixed distance of 2 mm and an area of 0.28
168 cm^2. A low frequency, non-actinic measuring beam and a 0.6 s saturation pulse of
169 ~8000 µmol m^{-2} s^{-1} photosynthetically available radiation (PAR) were used (*see* Table
170 1 for notation). The fluorometer photomultiplier signal gain was set at a level to ensure
171 fluorescence yields of >300 units for all measurements (with a new auto zero set each
172 time the gain was altered). The external irradiance levels were logged at each station
173 using the PAM light sensor. All data were stored and downloaded using WinControl-3
174 software.

175 The saturating pulse was applied to the sediments and the operational photosystem II
176 chl fluorescence yield in actinic light (F') was recorded. The fluorescent parameter F_m
177 (in the dark, first step of a rapid light curve) and F_m' (in the light, subsequent steps of a
178 rapid light curve), the maximum PSII chl fluorescence yield in actinic light when all
179 reaction centres are closed, are often underestimated (*see* Serôdio et al. 2005) due to
180 retained non-photochemical down regulation in the dark (Perkins et al. 2010).
181 Therefore, the maximum F_m' value ($F_{m'max}$), higher than F_m, measured under low actinic
182 light, is used for the calculation of associated photophysiological parameters (e.g.
183 NPQ, F_v/F_m, *see below*). The maximum quantum efficiency of PSII (F_q'/F_m') was
184 calculated as (F_m' – F')/F_m'. Rapid Light Curves (RLCs) were produced following
185 Perkins et al. (2006) for the determination of the maximum relative Electron Transport
186 Rate ($rETR_{max}$), light saturation coefficient (E_k) and the light use coefficient for PSII (α),
187 derived from curve fitting the model of Eilers & Peeters (1988) using Sigmaplot curve
188 fitter (Systat Software Inc., San Jose). RLCs consisted of the fluorescence responses
189 to nine different actinic irradiances of 20 s duration. The model consisted of an iterative
190 solution to the curve with 100 iterations processed and significant ($p<0.001$)

191   coefficients of a, b and c (Eilers & Peeters, 1988). Some individual RLCs saturated,

192   with these coefficients used to calculate $rETR_{max}$ and α. However, some RLCs failed

193   to saturate, therefore $rETR_{max}$ and E_k could not be calculated. $rETR_{max}$ was hence

194   estimated as the highest value at the end of the RLC and is used here as a proxy for

195   relative primary productivity. α was also calculated as the initial slope of the RLC simply

196   from:-

197    $α = (ΔrETR / ΔPAR)$ over the first two light curve steps.

198   The maximum quantum yield of PSII in the dark-adapted state, used as a proxy for

199   MPB biofilm health/nutrient limitation, F_v/F_m (Genty et al., 1989) was calculated as:-

200    $F_v/F_m = (F_{m\,max}' - F_o)/F_{m\,max}'$

201   The fluorescent parameters of $F_{m\,max}'$ and F_m' were used to calculate downregulation of

202   photochemistry (Lavaud, 2007), in the form of non-photochemical quenching (NPQ):-

203    $NPQ = ((F_{m\,max}' - F_m')/F_m')$.

204   Maximum NPQ (NPQ_{max}) was estimated from each light curve based upon the peak

205   NPQ value. Proportional changes of F' and F_m' were analysed to determine whether

206   diatoms were vertically migrating or undergoing NPQ reversal/induction (*see* Perkins

207   et al. 2010).

208   **Statistical analysis**

209   To determine the variability in biofilm mediation of Si between warm and cold periods,

210   the existence of significant difference ($p<0.001$) between summer and winter sampled

211   periods was tested. Data (BBSi, BDSi, $P-PO_4-$, chl *a* and water content) which failed

212   normal distribution (Kolmogorov Smirnov test) and homogeneity of variance (Levene's

213   test) was tested using Mann-Whitney U. Data ($rETR_{max}$ and irradiance levels) which

214   had normal distribution (Kolmogorov Smirnov test) and homogeneity of variance

215   (Levene's test) was tested using a Two-tailed Student's t-test. The significant ($p<0.05$)

216   variability between sites within each season was tested using a Kruskal-Wallis test and

217   one-way ANOVA. The relationship between biological variables and Si was tested,

218   with linear relationships assed using Pearson's correlations.

Results

219   **BBSi and BDSi intertidal mudflat standing stocks**

220   The Severn Estuary intertidal mudflats had low standing stocks of particulate Si in the

221   form of BBSi during the summer (0.6%) and winter (0.5%) sampled periods of 2014

222   (Fig. 2), compared to previous benthic Si estuarine studies (*e.g.* Chou & Wollast, 2006;

223   Arndt & Regnier, 2007). BBSi was significantly higher ($U_{df}=362.5$, $Z=-3.2118$, $p<0.001$)

224   under warm conditions compared to cold conditions. BBSi standing stocks were
225   significantly higher during the sampled summer ($H_{(2)}$=16.31, p<0.05) and winter
226   ($H_{(2)}$=23.2, p<0.05) periods at site 3, nearest to the marine zone, compared to other
227   sampled sites. As a result of local sediment conditions, BBSi varied spatially between
228   the sampled sites, with lower BBSi concentrations at sites 1 (high sand content)
229   compared to high concentrations at site 3 (high mud content), under both warm and
230   cold conditions (Fig. 3). Water content was significantly lower during the warm
231   ($H_{(2)}$=27.73, p<0.001) and cold ($H_{(2)}$=15.07, p<0.001) periods at Site 1 (exposed and
232   high sand content), compared to site 3 (sheltered and high mud content).

233   Si in the Severn Estuary was predominantly present in dissolved forms (Fig. 2). BDSi
234   concentrations in the mudflats were significantly greater (U_{df}=1, Z=-7.2815, p<0.001)
235   under relatively colder conditions (22.6 ± 1.0 mg L^{-1}) compared to relatively warm
236   conditions (2.9 ± 0.5 mg L^{-1}) (Fig. 2). Standing stocks of BDSi was greater at site 3
237   during the warmer summer, with concentrations averaging 4.2 ± 1.2 mg L^{-1} compared
238   to site 1 and 2 (*av.* 2.2 ± 0.4 mg L^{-1}). Under these warm conditions at site 1, chl *a*
239   positively correlated with BDSi (Table 3). The highest standing stock of BDSi was
240   recorded at site 1 during the colder winter period, near the mouth of the River Severn,
241   with concentrations averaging 24.7 ± 1.6 mg L^{-1}, potentially resulting from increased
242   river flow following high rainfall (Fig.2). Furthermore, BDSi positively correlated with
243   chl *a* during the winter sampled period (Table 3).

244   P-PO$_4^-$ concentrations were greatest during the relatively colder winter period (0.18 ±
245   0.02 mg L^{-1}) compared to the warm summer period (0.16 ± 0.02 mg L^{-1}) (Fig. 3), but
246   lacked significant variation. P-PO$_4^-$ sampled in the summer negatively correlated with
247   BBSi (Table 3). Furthermore, P-PO$_4^-$ concentrations were below detection level at site
248   3 during the summer period (Fig. 3).

249   **Biological mediation of Si**
250   The key diatom taxa observed under seasonal environmental differences were
251   *Pleurosigma, Gyrosigma and Nitzschia sigma*, similar to the findings presented by
252   Yallop et al. (1994) following an investigation of Portishead mudflats (site 2). Chl *a* was
253   significantly higher (U_{df}=176, Z=-5.3102, p<0.001) during cold conditions (240 ± 23 mg
254   g^{-1} *sed. dw.*) compared to warm conditions (132 ± 19 mg g^{-1} *sed. dw.*), with average air
255   temperatures having declined by 10.1°C (Fig. 2). Biofilm chl *a* sampled during the
256   summer, positively correlated with BBSi (Table 3). Chl *a* was higher at site 3 compared

257   to other sampled sites in both periods of the study (Table 2). Furthermore, at site 3,

258   under cold conditions, chl a positively correlated with BBSi (Table 3).

259   Variable chlorophyll fluorescence analysis during both warm and cold conditions was

260   measured over periods of approximately 3 hrs, with both photoperiods subject to high

261   irradiance levels, with peak values of 1278 µmol photons s^{-1} m^{-2} (summer) and 1944

262   µmol photons s^{-1} m^{-2} (winter). Diatoms exposed to warmer conditions were significantly

263   more productive (t(df)=5.6104, p<0.001) compared to diatoms exposed to colder

264   conditions, with $rETR_{max}$ averaging 254.1 ± 20.1 and 116.0 ± 27.1 rel. units,

265   respectively (Table 2), thus increasing the potential for biomineralization of Si under

266   warm conditions (Fig. 2) through enhanced rates of productivity. However, $rETR_{max}$ at

267   site 1, sampled during the summer, negatively correlated with BBSi but positively

268   correlated with BBSi in winter (Table 3). During cold conditions site 3, $rETR_{max}$

269   negatively correlated with BBSi (Table 3). Similar to $rETR_{max}$, α was higher during

270   warmer conditions compared to cold conditions (0.22 ± 0.1 and 0.18 ± 0.02 µmol

271   photons s^{-1} m^{-2}, respectively).

272   During both warm and cold periods, a high proportion of RLCs failed to saturate,

273   probably due to downward migration of cells away from the fluorometer light source as

274   light intensity increased (Fig. 4). In the summer sampling period, 94% of light curves

275   did not saturate, decreasing to 58% in the winter, suggesting a greater level of cell

276   movement under warm conditions. F_v/F_m (0.65 ± 0.08 and 0.44 ± 0.2 rel. units) and

277     $F_{m\,max}^{'}$ (2894 ± 614 and 1946 ± 272 rel. units) were higher under cold conditions

278   compared to the warmer ones, respectively (Table 2). However, the high irradiance

279   levels recorded during the winter sampling period, despite lower sunshine hours,

280   resulted in down regulation of both α and $rETR_{max}$, which implies reduced productivity

281   and hence reduced biomineralization of Si (Fig. 2).

282   As a response to high irradiance levels, the MPB biofilms performed both behavioural

283   and physiological downregulation in order to maximise photosynthesis. Biofilms

284   sampled during the summer were characterised by a migrational system (Fig. 4 and

285   5). Diatoms used downward cell movement away from increasing light levels during

286   the RLCs, increasing $F_q^{'}/F_m^{'}$ (Fig. 5). Additionally, as light levels increased there was a

287   rise in $F_m^{'}$ and F', indicating NPQ reversal alongside downward migration, causing a

288   decrease in these fluorescence yields. As NPQ would be induced with increasing light

289   levels, and Q_A would become reduced (both processes acting to reduce yields in the

290   case of F'), these data (F' and $F_m^{'}$ yields, NPQ data, Fig. 5) suggest downward vertical

291 cell movement, supporting this to be the cause for the lack of saturation of RLCs (*see*
292 *above*). It should be noted that, NPQ, sampled during the summer, positively
293 correlated with BBSi (Table 3), suggesting that these migratory biofilms were
294 sufficiently productive (higher $rETR_{max}$ and α compared to the sampled winter) to
295 mediate BBSi, despite having lower biomass.

296 Biofilms sampled during the winter were characterised by high NPQ induction as a
297 response to high irradiance, with reduced migration of the biofilms (Fig. 4 and 5), and
298 hence a larger proportion of RLCs saturated. Residual NPQ was observed at site 2
299 and 3 (Fig. 5) at the beginning of the RLCs. With increasing PAR, F_m' declined, and
300 NPQ and F' increased (Fig. 5), suggesting NPQ induction was greater, and downward
301 cell movement was reduced, compared to the summer. A lack of downward migration
302 was also supported by the larger decrease in F_q'/F_m' with increasing PAR increments
303 (Fig. 5). Furthermore, NPQ_{max} sampled during the winter was higher compared to that
304 sampled during summer (0.8 ± 0.5 and 0.19 ± 0.1 rel. units, respectively) and NPQ
305 positively correlated with $rETR_{max}$ (Table 3).

Discussion

307 Microphytobenthos (MPB) biofilms under warmer summer conditions had lower
308 biomass, and biologically mediated Si through the ecological function of the productive,
309 high light acclimated diatoms that were highly motile during fluorescence
310 measurements. This migratory behaviour increased the potential for growth and
311 the formation of biofilms, which initiated the build-up of BBSi. Biofilms subject to colder
312 winter conditions, had higher relative biomass but of low light acclimated diatoms,
313 which had reduced migratory capabilities and induced NPQ throughout the
314 photoperiod. Through the reduced rates of productivity the potential for
315 biomineralization of Si may have been reduced. However, despite the high
316 photosynthetic abilities of the diatoms, and regardless of different temperature
317 regimes, the biological mediation of BBSi was low, with poor BDSi uptake, typical of
318 biofilms in a dynamic intertidal estuary subject to high re-suspension and tidal
319 influences. These dynamics resulted in low mudflat BBSi standing stocks, with
320 estuarine Si dominated by dissolved forms, especially during cold periods with
321 increased rainfall. In summary, environmental conditions influenced the diatom-
322 dominated MPB biofilm biological mediation of Si, preventing sufficient accumulation
323 of BBSi in the intertidal mudflats of the Severn Estuary. Therefore, BBSi and BDSi

324 concentrations were best explained by complex hydrodynamics, dissolution kinetics
325 and terrestrial/coastal inputs rather than the biological uptake of Si.

326 **BBSi and BDSi in the Severn Estuary**
327 Low BBSi standing stocks in the intertidal mudflats were observed during the summer
328 (0.6%) and winter (0.5%) sampled periods (Fig. 2). The Severn Estuary may have a
329 low BBSi retention throughout the year (Fig. 6), similar to previous benthic Si estuarine
330 studies (Ragueneau et al. 1994; Arndt & Regnier, 2007; Arndt et al. 2007; Jacobs,
331 2009; Laurelle et al. 2009; Carbonnel et al. 2009; 2013; Raimonet et al. 2013). For
332 example, Chou & Wollast (2006) report low BBSi standing stocks in the Scheldt
333 between 0.05% and 1.5%. Estuarine BSi and BBSi budgets are often low due to the
334 hydro-geomorphological processes enhancing turbidity, leading to a reduction in the
335 abundance of photosynthetic diatoms (Tréguer & De La Rocha, 2013). However, the
336 high BDSi standing stocks (Fig. 2) suggest that the estuary can be considered as an
337 efficient filter for DSi and may have a significant importance regarding Si cycling.

338 The spatial distribution of BBSi between the three sites (Fig. 6) reflected three
339 processes; (1) settlement and biological accumulation of particulates relative to the
340 estuarine hydrodynamics, inducing the retention of Si in more sheltered locations, (2)
341 transportation of particulates as suspended material downstream, and (3) dissolution
342 at biological timescales. Sediment dynamics were likely different at each sampled site.
343 For example, the exposed mudflats at site 1 likely experienced high rates of erosion
344 and re-suspension, which reduced BBSi standing stocks (Fig. 3), whereas the
345 sheltered mudflats from the prevailing south westerly winds at site 3 had increased
346 deposition, inducing the build-up of biofilms, and subsequently BBSi (Fig. 3). However,
347 the overall low standing stocks of BBSi (Fig. 2) suggests the overall high rates of re-
348 suspension in the estuary (Manning et al. 2010), preventing the settling and
349 accumulation of particulates in the high water content intertidal mudflats (Table 2),
350 coinciding with the hyper-tidal regime (Neill & Couch, 2011), were the most likely
351 candidates to explain the observed variations in BBSi. This increased transport of BBSi
352 to the pelagic zone may support high primary productivity in the marine zone of the
353 Outer Bristol Channel (Morris, 1984).

354 The combination of high suspended particulate matter (SPM) and turbidity maxima,
355 further explain the low mudflat BBSi concentrations. Sediment dynamics have
356 previously been investigated for the Severn Estuary (Allen, 1990; Duquesne et al.
357 2006; Jonas & Millward, 2010). Manning et al. (2010) report of a turbidity maximum,

358   where SPM concentrations were in excess of 10 g L^{-1} in the upper estuary near site 2,
359   which may have reduced chl *a* (Table 2) and subsequently BBSi (Fig. 3). The
360   contribution of BBSi from the re-suspended sediments to the overall estuarine BSi
361   budget remains unknown. Previous studies have estimated between 20% and 40% of
362   biofilms are re-suspended (de Jonge & van Beusekom, 1992, 1995; Hanlon et al.
363   2006). Considering the expected high re-suspension rates and sediment loads, along
364   with the pelagic fraction of BSi, which is expected to be small (Underwood, 2010), the
365   overall estuarine system is unlikely to have a significant retention of BSi, despite
366   potentially high terrestrial inputs of Si (*e.g.* DeMaster, 1981; Muylaert & Raine, 1999).
367   However, a large variation in BBSi resuspension would be expected between spring
368   and neap tides. For example, Parker & Kirby (1981) report 70% of the sediment placed
369   into suspension on a spring tide is settled on a neap tide.

370   Dissolution kinetics may also explain the variations in Si between the three sampled
371   sites (Fig. 3), where particulates were transported downstream, gradually dissolving,
372   increasing BDSi concentrations (*e.g.* De'Elia et al. 1983; Yamada & De'Elia 1984).
373   Spatial variations in nitrate, ammonium, phosphate and silicate have previously been
374   shown in the estuary between the freshwaters end members (*av.* 2.7‰) to the marine
375   end members (*av.* 28.3‰) (Underwood, 2010). Similarly, in the Bay of Brest (Beucher
376   et al. 2004) and in Chesapeake Bay (De'Elia et al. 1983), BSi dissolution increased
377   DSi retention to 48% and 65%, respectively. The Severn Estuary may exhibit similar
378   characteristics to the Oder Estuary, including (1) higher export of Si compared to
379   retention, (2) BBSi dissolution resulting in high BDSi retention, and (3) Si fractions
380   dominated by dissolved forms. For example, Pastaszuak et al. (2008) suggests the
381   Oder Estuary behaved as a source of DSi through the dissolution of ~50% of BSi into
382   DSi, with 25% of BSi transported to a nearby Bay.

383   Terrestrial discharge was likely the primary environmental factor influencing the
384   distribution and concentration of Si, and likely influenced the biofilm biological
385   mediation of Si. For example, at the mouth of the River Severn (site 1), the highest
386   standing stock of BDSi was recorded with concentrations averaging 24.7 ± 1.6 mg L^{-1},
387   which correlated with high chl *a* content (Table 3). However, Morris (1984) note the
388   River Severn only supplies a quarter of the freshwater into the estuary. Dissolution of
389   Si may have been less significant compared to terrestrial inputs, especially during the
390   cold winter season (Fig. 2). For example, dissolution in the Scheldt Estuary was of
391   minor importance (3.6%) compared to the riverine influx of DSi (5.9×10^7 mol) (Arndt &
392   Regnier, 2007). Terrestrial inputs likely resulted in high BDSi concentrations (Fig. 2),

393 especially during the winter following high rainfall in the Severn Estuary catchment
394 area (273. 5 mm; Met Office, 2015) (Fig. 2). High winter Si concentrations have
395 previously been recorded for the estuary (Morris, 1984). In contrast, during the
396 summer, lower rainfall (103.8 mm; Met Office, 2015) (Fig. 2) alongside peak biological
397 activity (Table 2), likely reduced BDSi standing stocks, and led to a rise in BBSi (Fig.
398 2).

399 Terrestrial inputs may also have increased the supply of detrital BSi (BSi_{det}), e.g.
400 phytoliths (Conley, 2002). For example, saltmarshes and wetlands have been shown
401 (Norris & Hackney, 1999) to have significant *in situ* accumulation of phytolith BSi. BSi_{det}
402 originating from these habitats may have been responsible for significantly ($p<0.001$)
403 higher BBSi concentrations (Fig. 3) and chl *a* contents (Table 2), and the significant
404 correlations between chl *a* and $rETR_{max}$ with BBSi at site 3 (Table 3). Furthermore,
405 BSi_{det} from the river and saltmarshes may have contributed as a source of BDSi via
406 remineralization through pore and groundwater discharge by advective transport at
407 high tide, and seepage at low tide (Georg et al. 2009), with phytolith dissolution proven
408 to double DSi inputs compared to dissolution from silicate mineral weathering (Struyf
409 et al. 2005).

Biological mediation of Si

411 *MPB biomass and productivity*
412 MPB biomass exhibited a significant ($p<0.001$) difference between warmer summer
413 conditions (13.2 mg g^{-1} *sed. dw.*) and colder winter conditions (24.0 mg g^{-1} *sed. dw.*)
414 (Table 2). The low winter temperatures (Fig. 2) may have reduced diatom metabolism
415 and/or inhibited cell movement through extracellular polymers (EPS), restricting
416 diatoms ability to vertically migrate away from the fluorometer light source as light
417 intensity increased, subsequently increasing the cell biomass in the surficial 5 mm.

418 Biomass was high compared to previous estuarine studies (*e.g.* Underwood &
419 Kromkamp, 1999) and previous studies on the Severn Estuary (*e.g.* Underwood &
420 Paterson, 1993; Yallop & Paterson, 1994) possibly reflecting increased cohesivity
421 (enhanced by biostabilization), and favourable conditions necessary for benthic
422 growth. Therefore, sites with high water content, e.g. site 2 in the sampled winter
423 (Table 2), may have increased re-suspension rates, reducing the biofilm biomass and
424 accumulation of BBSi (Fig. 3). However, during a tidal emersion period where
425 sediments undergo desiccation due to de-watering, sediment of a lower water content
426 may actually exhibit lower chl *a* content per unit weight of sediment due to an increase

427   in sediment bulk density, emphasising the importance to incorporate changes in water

428   content into the calculation of chl *a* content (*see* Perkins et al. 2003). The change in

429   sediment cohesivity between the summer and winter sampling periods likely influenced

430   the variation in biofilm relative primary productivity. The biofilms sampled during the

431   summer had high water content, and were highly productive with relative primary

432   productivity averaging highs of 254.1 ± 20.1 rel. units, despite having lower biomass.

433   In comparison, biofilms sampled during the colder winter period were of a lower water

434   content, and had reduced rates of relative primary productivity (116.0 ± 27.1 rel. units),

435   despite higher biomass (Table 2). However, the complex hydrodynamics most likely

436   resulted in a constant turnover of the thin, unstable biofilms (Yallop et al. 1994), in line

437   with an active transient biofilm that reduced the ecological potential to accumulate

438   BBSi (Fig. 2). Chl *a* positively correlated with BBSi, consistent with a decline in BBSi

439   concentrations corresponding to reduced biomass of the diatom-dominated biofilms

440   (Table 3).

441   The study assumed the measured chl *a* was unique to diatoms, however it was

442   possible that BSi_{det} and higher abundances of green algae, euglenophytes and

443   cyanobateria (Oppeneheim, 1998, 1991; Underwood, 1994) may have influenced chl

444   *a* and BBSi measurements. Previous studies (Oppenheim, 1988, 1991) have shown a

445   total of 65 taxa, with MPB composition primarily of *N. vacilla*, *Navicula viridula var.*

446   *rostellata*, *N. humerosa* and *Diploneis littoralis*. Furthermore, diatoms having greater

447   migratory behaviours, for example the observed *Pleurosigma*, may have reduced the

448   surficial biomass and the biofilms rates of productivity (Cartaxana et al. 2011).

449   *Photosynthetic ability of MPB biofilms*

450   Biofilms subject to warmer summer conditions were significantly ($p<0.001$) more

451   productive and efficient compared to those subject to colder winter conditions, and

452   exhibited strong migratory behaviour (Fig. 5). This behaviour has previously been

453   observed in diatom-dominated biofilms (Perkins et al. 2010). MPB sampled during the

454   summer exhibited higher α and $rETR_{max}$ (Table 2) with data (F', F_m' yields, and NPQ,

455   Fig. 5) suggesting downward migration was dominant, causing the lack of RLC

456   saturation (Fig. 4). Indeed, 94% of the RLCs did not saturate. As a result of the

457   enhanced rates of productivity there was greater biological mediation of Si and higher

458   BBSi mudflat standing stocks in the sampled summer period (Fig. 2). A lack of RLC

459   saturation on natural samples has previously been measured (Kromkamp et al. 1998;

460   Perkins et al. 2002; 2010a). Comparative studies (Perkins et al. 2002; 2010b; Serôdio

461 et al. 2006a; 2008) have also shown migration to follow NPQ induction as diatoms
462 acclimate to increasing light levels.

463 Diatoms sampled during the warmer summer period were relatively nutrient limited,
464 with low F_v/F_m recorded at all sample sites (Table 2), correlating with BBSi (Table 3).
465 For example, P-PO$_4^-$ was below the detection level at site 3 (Fig. 3). However, P-PO$_4^-$
466 negatively correlated with BBSi (Table 3), suggesting at high P-PO$_4^-$ concentrations,
467 BDSi became limiting, potentially as a result of peak summer biological activity. Low
468 standing stocks of BDSi have also been recorded in the Oder Estuary during peak
469 diatom activity in the spring and summer, alongside low DSi riverine loads (which
470 neared 0 µmol dm^{-3}) (Pastuszak et al. 2008).

471 The significant ($p<0.001$) difference between biofilm productivity measured during the
472 summer and winter sampled periods was best explained by higher peak irradiance
473 levels experienced during the winter photoperiod, resulting in downregulation (mainly
474 in the form of NPQ induction) of both α and rETR$_{max}$ (Table 2) which led to reduced
475 productivity and the reduced biological mediation of Si. NPQ$_{max}$ was higher during cold
476 conditions (0.8 ± 0.5 rel. units) compared to warmer ones (0.2 ± 0.07 rel. units) and
477 considered in line with typical NPQ$_{max}$ values below 4.0 rel. units (Serôdio et al. 2005).
478 Furthermore, NPQ positively correlated with rETR$_{max}$ (Table 3), suggesting NPQ
479 induction likely influenced winter productivity. Diatoms sampled during the colder
480 winter period were not nutrient limited (high F_v/F_m), but were acclimated to low light
481 and had restricted migrational activity. This contributed to the large reduction in F_q'/F_m'
482 with increasing PAR, and resulted in a higher proportion (42%) of RLCs saturating
483 (compared to 6% in summer), e.g. at site 2 and 3 (Fig. 4). Therefore, temperature was
484 likely a key factor in determining the balance between behavioural and physiological
485 down regulation of photochemistry. However, inflections in RLCs (see Perkins et al.,
486 2001) were observed during the winter at site 2 and 3, between irradiance levels of
487 579-803 and 283-411 µmol photons s^{-1} m^{-2}, respectively (Fig. 4). These S-shaped
488 curves have occasionally been observed in in situ measurements of intact sediment
489 (Perkins et al. 2002) and suggest vertical migration. Further, the large difference in
490 PAR at which the inflections occurred may have also resulted from different diatom
491 communities present.

Conclusions

The extensive intertidal mudflats of the hypertidal Severn Estuary are an ideal study areas to carry out a multidisciplinary analysis of Si, allowing for a comprehensive examination of estuarine internal Si cycling. Here we show environmental factors to influence the diatom-dominated biofilms ability to mediate Si. BBSi standing stocks in the mudflats were low compared to other European estuaries. Dissolved Si forms dominated the estuary, with BDSi concentrations reflecting both biological mediation with near complete consumption during the warmer summer conditions, as well as terrestrial/coastal inputs. Biofilms subject to warmer conditions biologically mediated Si by the productive, low biomass of high light acclimated diatoms that were highly motile during fluorescence measurements. This migratory behaviour, despite nutrient limitation, increased the potential for growth and the accumulation of BBSi. Biofilms subject to colder winter conditions of a higher relative biomass of low light acclimated diatoms, had reduced migratory capabilities and induced NPQ throughout the photoperiod. The potential for biomineralization of Si was scaled down as a result of lower rates of productivity under colder winter conditions. We conclude that temperature was an important driver of biofilm productivity. However, despite the high photosynthetic abilities of the diatoms, the biological mediation of BBSi was considered low during both sampled periods. BBSi and BDSi concentrations were best explained by complex hydrodynamics increasing biofilm re-suspension, dissolution kinetics and terrestrial/coastal inputs rather than the biological uptake of Si. However, the estuaries importance for Si cycling on a wider geographical scale, considering the high BDSi standing stocks, high rates of re-suspended BBSi and all external inputs of Si, requires further work into, 1) the benthic-pelagic coupling, 2) transportation of Si and nutrients along the tidal river, estuary and coastal zone, and 3) the influence of the complex tidal regime and sediment dynamics (through re-suspension and mineralization) on Si over spatial and temporal scales.

Acknowledgments

References

Allen, J. 1990. The Severn Estuary in southwest Britain: its retreat under marine transgression, and fine-sediment regime. *Sedimentary Geology.* 66:13–28.

Arndt, S., Regnier, P. 2007. A model for the benthic-pelagic coupling of silica in estuarine ecosystems: sensitivity analysis and system scale simulation. *Biogeosciences.* 4:331–352.

Arndt, S., Vanderborght, J., Regnier, P. 2007. Diatom growth response to physical forcing in a macrotidal estuary: Coupling hydrodynamics, sediment transport, and biogeochemistry. *J. Geophys. Res.* 112.

Aure, J., Danielssen, D., Svendsen, E. 1998. The origin of Skagerrak coastal water off Arendal in relation to variations in nutrient concentrations. *ICES J. Mar. Sci.* 55:610 – 619.

Beucher, C., Tréguer, P., Corvaisier, R., Hapette, A., Elskens, M. 2004. Production and dissolution of biosilica, and changing microphytoplankton dominance in the Bay of Brest (France). *Mar Ecol Prog Ser.* 267:57-69.

Brzezinski, M., Villareal, T., Lipschultz, F. 1998. Silica production and the contribution of diatoms to new and primary production in the Central North Pacific. *Mar. Ecol.: Prog. Ser.* 167:89–104.

Carbonnel, V., Lionard, L., Muylaert, K., Chou, L. 2009. Dynamics of dissolved and biogenic silica in the freshwater reaches of a macrotidal estuary (The Scheldt, Belgium). *Biogeochemistry.* 96:49–72.

Carbonnel, V., Vanderborght, J., Chou, L. 2013. Silica Mass-Balance and Retention in the Riverine and Estuarine Scheldt Tidal System (Belgium/The Netherlands). *Aquatic Geochemistry.* 19:501-516.

Cartaxana, P., Ruivo, M., Hubas, C., Davidson, I., Serôdio, J., Jesus, B. 2011. Physiological verses behavioural photoprotection in intertidal epipelic and epipsamic benthic diatom communities. *Journal of Experimental Marine Biology Ecology.* 405:120-127.

Conley, D., Malone, T. 1992. Annual cycle of dissolved silicate in Chesapeake Bay: implications for the production and fate of phytoplankton biomass. *Marine Ecology Progress Series.* 81:121-128.

Conley, D. 2002. Terrestrial ecosystems and the global biogeochemical silica cycle. *Global Biogeochemical Cycles.* 16(4):68-75.

Correll, D., Jordan, T., Weller, D. 2000. Dissolved silicate dynamics of the Rhode river watershed and estuary. *Estuaries.* 23:188-198.

Chou, L., Wollast, R. 2006. Estuarine silicon dynamics, in: The Silicon Cycle: Human Perturbations and Impacts on Aquatic Systems, edited by: Ittekkot, D., Unger, C., Humborg, C., and Tac An. Island Press, Washington, Covelo, London. 66:93-120.

DeMaster, D. 1981. The supply and accumulation of silica in the marine environment. *Geochimica et Cosmochimica Acta.* 45:1715-1732.

De'Elia, C., Nelson, D., Bonton, W. 1983. Chesapeake Bay nutrient and plankton dynamics: III. The annual cycle of dissolved silicon. *Geochim Cosmochim Acta.* 47:1945-1955.

de Jonge, V., van Beusekom, J. 1992. Contributions of re-suspended microphytobenthos to total phytoplankton in the Ems estuary and its possible role for grazers. *Netherlands Journal of Sea Research.* 30:91–105.

de Jonge, V., van Beusekom, J. 1995. Wind- and tide-induced resuspension of sediment microphytobenthos from the tidal flats in the Ems estuary. *Limnology and Oceanography.* 40:766–778.

Duquesne, S., Newton, L., Giusti, L., Marriott, S., Stark, H., Bird, D. 2006. Evidence for declining levels of heavy-metals in the Severn Estuary and Bristol Channel, UK and their spatial distribution in sediments. *Environmental Pollution.* 143:187–196.

580   Eilers, P., Peeters, J. 1988. A model for the relationship between light intensity and the
581   rate of photosynthesis in phytoplankton. *Ecological Modelling.* 42:199-215.

582   Fortner, S.,Lyons, W., Carey, A., Shipitalo, M., Welch, S., Welch, K. 2012. Silicate
583   weathering and CO_2 consumption within agricultural landscapes, the Ohio-
584   Tennessee River Basin, USA S. K. *Biogeosciences.* 9:941-955.

585   Genty, B., Briantais, J., Baker, N. 1989. The relationship between the quantum yield
586   of photosynthetic electron transport and quenching of chlorophyll
587   fluorescence. *Biochimica et Biophysica Acta.* 990:87-92.

588   Georg, R., West, A., Basu, A., Halliday, A. 2009. Silicon fluxes and isotope composition
589   of direct groundwater discharge into the Bay of Bengal and the effect on the
590   global ocean silicon isotope budget. *Earth and Planetary Science Letters.*
591   283:67-74.

592   Gilpin, L., Davidson, K., Roberts, E. 2004. The influence of changes in nitrogen: silicon
593   ratios on diatom growth dynamics. *Journal of Sea Research.* 51:21-35.

594   Hammer, O., Harper, D., Ryan, P. 2001. PAST: Paleontological statistics software
595   package for education and data analysis. [online] Available in: <http://palaeo-
596   electronica.org/2001_1/past/issue1_01.htm>.

597   Hanlon, A., Bellinger, B., Haynes, K., Xiao, G., Hofmann, T., Gretz, M., Ball, A.,
598   Osborn, A., Underwood, G. 2006. Dynamics of extracellular polymeric
599   substance (EPS) production and loss in an estuarine, diatom-dominated,
600   microalgal biofilm over a tidal emersion-immersion period. *Limnology and
601   Oceanography.* 21:79–93.

602   Hurd, D. 1977. The effects of glacial weathering on silica budget of Antarctica waters.
603   *Geochim Cosmochim Acta.* 41:1213-1222.

604   Jacobs, S. 2009. Silica cycling and vegetation development in a restored freshwater
605   tidal marsh. 1-198.

606   Jesus, B., Perkins, R., Consalvey, M., Brotas, V., Paterson, D. 2006. Effects of vertical
607   migrations by benthic microalgae on fluorescence measurements of
608   photophysiology. *Marine Ecology Progress Series.*315:55–66.

609   Jonas, P., Millward, G. 2010. Metals and nutrients in the Severn Estuary and Bristol
610   Channel: contemporary inputs and distributions. *Marine Pollution Bulletin.*
611   61(1-3):52-67.

612   Kromkamp, J., Barranguet, C., Peene, J.1998. Determination of microphytobenthos
613   PSII quantum efficiency and photosynthetic activity by means of variable
614   chlorophyll fluorescence. *Marine Ecology Progress Series.* 62:45–55.

615   Kirby, 2010. Distribution, transport and exchnages of fine sediment, with tidal power
616   implications: Severn Estuary, UK. *Marine Pollution Bulletin.* 61:21-36.

617   Lavaud, J., Kroth, P. 2006. In diatoms, the transthylakoid proton gradient regulates the
618   photoprotective non-photochemical fluorescence quenching beyond its control
619   on the xanthophyll cycle. *Plant Cell Physiol*ogy. 47:1010-1016.

620   Lavaud, J. 2007. Fast regulation of photosynthesis in diatoms: mechanisms, evolution
621   and ecophysiology. *Plant Science and Biotechnology.* 1:267-287.

622   Liang, D., Junqiang, X., Falconer, R., Zhang, J. 2013. Study on Tidal Resonance in
623   Severn Estuary and Bristol Channel. *Coastal Engineering Journal.* 56(1):1-18.

624   Liu, W., Hsu, M., Chen, S., Wu, C., Kuo, A. 2005. Water column light attenuation
625   Dasnshuei river estuary, Taiwan. *Journal of the American Water Resource
626   Association.* 425-435.

627   Liu, S., Ye, X., Zhang, L., Zhang, G., Wu, Y. 2008. The silicon balance in Jiaozhou
628   Bay, North China. *J Mar Syst.* 74:639-648.

629   Liu, S., Hong, G., Zhang, J., Ye, X., Jiang, X. 2009. Nutrient budget of large Chinese
630   estuaries. *Biogeosciences.* 6:2245-2263.

631   Lorenzen, C. 1966. A method for the continuous measurement of in vivo chlorophyll
632   concentration. *Deep-Sea Research.* 13: 223-227.

633   Manning, A., Langston, W., Jonas, P. 2010. A review of sediment dynamics in the
634   Severn Estuary: Influence of flocculation. *Marine Pollution Bulletin.* 61:37–51.

Maxwell, K., Johnson, G. 2000. Chlorophyll fluorescence-a practical guide. *Journal of Experimental Botany.* 51:659–668.

Met Office. 2011. Climate: Observations, projections and impacts. [pdf] Met Office. Available in: <http://www.metoffice.gov.uk/media/pdf/t/r/UK.pdf> [Accessed 2015].

Met Office. 2015. UK climate: download regional values. [pdf] Met Office. Available in: <http://www.metoffice.gov.uk/climate/uk/summaries/datasets> [Accessed 2015].

Moosdorf, N., Hartmann, J., Lauerwald, R. 2011. Changes in dissolved silica mobilization into river systems draining North America until the period 2081–2100. *Journal of Geochemical Exploration.* 110(1):31-39.

Morris, R. 1984. The chemistry of the Severn Estuary and the Bristol Channel. *Marine Pollution Bulletin.* 15(2):57-61.

Muylaert, K., Raine, R. 1999. Import, mortality and accumulation of coastal phytoplankton in a partially mixed estuary (Kinsale harbour, Ireland). *Hydrobiologia.* 412:53-65.

Norris, A., Hackney, C. 1999. Silica content of a mesohaline tidal marsh in North Carolina. *Estuarine Coastal Shelf Science.* 49:597-605.

Neill, S., Couch, S. 2011. Impact of Tidal Energy Converter (TEC) array operation on sediment dynamics. *Renewable Energy.* 37:387-397.

Oppenheim, D. 1988. The distribution of epipelic diatoms along an intertidal shore in relation to principal physical gradients. *Botanica Marina.* 31:65–72.

Oppenheim, D. 1991. Seasonal changes in epipelic diatoms along an intertidal shore, Berrow flats, Somerset. *Journal of the Marine Biological Association of the United Kingdom.* 71:579–596.

Parker, W., Kirby, R. 1981. The behaviour of cohesive sediment in the inner Bristol Channel and Severn Estuary in relation to construction of the Severn Barrage (Unpublished). *Institute of oceanographic sciences.* 117: 1-39.

Pastuszak, M., Conley, D., Humborg, C., Witek, Z., Sitek, S. 2008. Silicon dynamics in the Oder estuary, Baltic Sea. *Journal Marine System.* 73:250-262.

Perkins, R., Underwood, G., Brotas, V., Snow, G., Jesus, B., Ribeiro, L. 2001. Responses of microphytobenthos to light: primary production and carbohydrate allocation over an emersion period. *Marine Ecology Progress Series.* 223:101–12.

Perkins, R., Oxborough, K., Hanlon, A., Underwood, G., Baker, N. 2002. Can chlorophyll fluorescence be used to estimate the rate of photosynthetic electron transport within microphytobenthic biofilms? *Marine Ecology Progress Series.* 228:47–56.

Perkins, R., Honeywill, C., Consalvey, M., Paterson, D. 2003. Changes in microphytobenthic chlorophyll *a* and EPS resulting from sediment compaction due to de-watering: opposing patterns in concentration and content. *Continental shelf science.* 23(6):575-586.

Perkins, R., Mouget, J., Lefevre, S. 2006. Light response curve methodology and possible implications in the application of chlorophyll fluorescence to benthic diatoms. *Marine Biology.* 149:703-712.

Perkins, R., Lavaud, J., Mouget, S., Cartaxana, P., Rosa, P., Barille, L., Brotas, V., Jesus, B. 2010a. Vertical cell movement is a primary response of intertidal benthic biofilms to increasing light dose. *Marine Ecology Progress Series.* 416:93-103.

Perkins, R., Kromkamp, J., Serôdio, J., Lavaud, J., Jesus, B., Mouget, J., Lefebvre, S., Forster, R. 2010b. The application of variable chlorophyll fluorescence to microphytobenthic biofilms. In: Suggett, D., Borowitzka, M., Prášil, O. eds. *Chlorophyll a Fluorescence in Aquatic Sciences: Methods and Applications.* Developments in Applied Phycology. London: Springer. 4:237-275.

690 Pickney, J., Zingmark, R. 1991. Effects of tidal stage and sun angles on intertidal
691 benthic microalgae productivity. *Marine Ecology progress Series.* 76:81-89.
692 Raimonet, M., Andrieux,L., Ragueneau, O., Michaus, E., Kerouel, R., Philippon, X.,
693 Nonent, M., Laurent, M. 2013. Strong gradient of benthic biogeochemical
694 processes along a macrotidal temperate estuary: focus on P and Si cycles.
695 *Biogeochemistry. 115:399-417.*
696 Ragueneau O, De Blas Varela E, Tréguer P, Quéguiner B, Del Amo Y. 1994.
697 Phytoplankton dynamics in relation to the biogeochemical cycle of silicon in a
698 coastal ecosystem of western Europe. *Mar Ecol Prog Ser.* 106:157–172.
699 Ragueneau, O., Tréguer, P., Leynaert, A., Anderson, R., Brzezinski, M., DeMaster, D.,
700 Dugdale, R., Dymond, J., Fischer, G., Francois, R., Heinze, C., Maier-Reimer,
701 E., Martin-Jézéquel, V., Nelson, D., Quéguiner, B. 2000. A review of the Si
702 cycle in the modern oceans: recent progress and missing gaps in the
703 application of biogenic opal as a paleoproductivity proxy. *Global Planet*
704 *Change.* 26(4): 317-365.
705 Redfield, A., Ketchum, B., Richards, F. 1963. The influence of organisms on the
706 composition of sea water in the sea. 2:26-77.
707 Rendell, A, Horrobin, T., Jickells, T., Edmunds, H., Brown, J., Malcom, S. 1997.
708 Nutrient cycling in the Great Ouse estuary and its impact on nutrient fluxes to
709 The Wash, England. *Estuar Coast Shelf Sei.* 45(5):653-668.
710 Serôdio, J., Cruz, S., Vieira, S., Brotas, V. 2005. Non-photochemical quenching of
711 chlorophyll fluorescence and operation of the xanthophyll cycle in estuarine
712 microphytobenthos. *Journal of Experimental Marine Biology Ecology.* 326:157-
713 169.
714 Serôdio, J., Vieira, S., Cruz, S., Coelho, H. 2006a. Rapid light response curves of
715 chlorophyll fluorescence in microalgae: relationship to steady-state light curves
716 and non-photochemical quenching in benthic diatom-dominated assemblages.
717 *Photosynthesis Research.* 90:29–43.
718 Serôdio, J., Coelho, H., Vieira, S., Cruz, S. 2006b. Microphytobenthos vertical
719 migratory photoresponse as characterised by light-response curves of surface
720 biomass. *Estuarine Coastal and Shelf Science.* 68:547-556.
721 Serôdio, J., Vieira, S., Cruz, S. 2008. Photosynthetic activity, photoprotection and
722 photoinhibition in intertidal microphytobenthos as studied in situ using variable
723 chlorophyll fluorescence. *Continental Shelf Research.* 28:1363-1375.
724 Shwartz, S., Lorenzo, T. 1990. Chlorophyll in foods. *Food Science and Nutrition.*
725 29(1):1-17.
726 Smith, D., Underwood, G. 1998. Exopolymer production by intertidal epipelic diatoms.
727 *Limnol. Oceanogr.* 43(7): 1578-1591.
728 Struyf, E., Damme, S., Gribsholt, B., Meir, P. 2005. Freshwater marshes as dissolved
729 silica recyclers in an estuarine environment (Schelde estuary, Belgium).
730 *Hydrobiologia.* 540:69–77.
731 Teasdale, P., Batley, G., Apte, S., Webster, I. 1995. Pore water sampling with sediment
732 peepers. *Trends Anal. Chem.* 14:250–256.
733 Tréguer, P., De La Rocha, C. 2013. The World Ocean Silica Cycle. *Marine Science.*
734 5(5.1):2-25.
735 Underwood, G. 1994. Seasonal and spatial variation in epipelic diatom assemblages
736 in the Severn Estuary. *Diatom Research.* 9:451-472.
737 Underwood, G., Kromkamp, J. 1999. Primary production by phytoplankton and
738 microphytobenthos in estuaries. *Advance in Ecology Press.* 29:93–153.
739 Underwood, G. 2010. Microphytobenthos and phytoplankton in the Severn Estuary,
740 UK: Present situation and possible consequences of a tidal energy barrage.
741 *Marine Pollution Bulletin.* 61:83–91.
742 Underwood, G., Paterson, D.1993. Recovery of intertidal benthic diatoms from biocide
743 treatment and associated sediment dynamics. *Journal of the Marine Biological*
744 *Association of the United Kingdom.* 73:25–45.

745 West, A., Galy, A., Bickle, M. 2005. Tectonic and climatic controls on silicate
746   weathering. *Earth and Planetary Science Letters*. 235:211–228.
747 Yamada, S., De'Elia, C. 1984. Silicic acid regeneration from estuarine sediment cores.
748   *Marine Ecology Progress Series*. 18:113-118.
749 Yallop, M., Winder, B., Paterson, D., Stal, L. 1994. Comparative structure, primary
750   production and biogenic stabilization of cohesive and non-cohesive marine
751   sediments inhabited by microphytobenthos. *Estuarine, Coastal and Shelf*
752   *Science*. 39(6):565-582.
753 Yallop, M., Paterson, D. 1994. Survey of Severn estuary. In: Krumbein, W., Paterson,
754   D., Stal, L.(Eds.), Biostabilization of Sediments. Bibliotheks und
755   Informationssystem der Universität Oldenburg (BIS). Verlag, Oldenburg, pp.
756   279–326.

Figure Captions

Figure 1. Severn Estuary intertidal mudflat study area. Severn Estuary (A) is situated in the southwest of UK (B). Tidal limit in the River Severn reaches Maisemore, north Gloucester. Outer Severn Estuary limit identified as a transect between Lavernock Point and Sand Point (14 km wide), near Weston-Super-Mare. Mudflats north of Severn Bridge are sandy, whilst lateral banks south of the bridge are predominantly muddy. Estuary discharges into Bristol Channel followed by the Irish Sea and the North Atlantic Ocean. Bathymetry of the Severn Estuary (C). DTM of the coastline around the Severn Estuary (D).

Figure. 2. Standing stocks of BDSi (A) and BBSi (B) in the Severn Estuary intertidal mudflats. Rainfall (mm) for the Severn Estuary catchment area and average air temperature (°C) for the summer and winter sampled months (Met Office, 2015). Error bars are the standard error in the calculation of the average BDSi and BBSi concentration, rainfall and temperature. BBSi: benthic biogenic silica, n=36(summer), n=35(winter). BDSi: benthic dissolved silicon, n=36(summer), n=36(winter).

Figure. 3. Distribution of BDSi and BBSi during the summer (A) and winter (B), and P-PO_4^- concentration (C) in the Severn Estuary from the upper estuary (Severn Beach, site 1), to the mid-estuary (Portishead, site 2) and the lower mid-estuary (Newport Wetlands, site 3). Error bars are the standard error in the calculation of the average BDSi, BBSi and P-PO_4^- concentration. BBSi: benthic biogenic silica, n=36(summer), n=35(winter). BDSi: benthic dissolved silicon, n=36(summer), n=36(winter). P-PO_4^-: orthophosphate, n=36(summer), n=36(winter).

779 **Figure. 4.** Rapid Light Curves for the summer (A) and winter (B). Downregulation
780 interference (S-shaped) curves in winter RLCs at site 3 (light grey) and site 2 (dark
781 grey).

782 **Figure. 5.** Diatom photosynthetic activity and downregulation processes. A-C)
783 Summer chlorophyll fluorescence. D-F) Winter chlorophyll fluorescence. A and D) Site
784 1: $n=11$, $n=10$. B and E) Site 2: $n=11$, $n=5$. C and F) Site 3: $n=11$, $n=3$. Chlorophyll
785 fluorescence (F$'$ and F$_m'$). F$'$: minimum fluorescence yield in actinic light. F$_m'$: maximum
786 fluorescence yield in actinic light. PSII efficiency (F$_q'$/F$_m'$): maximum photosynthetic
787 efficiency of PSII. NPQ: non-photochemical quenching. PAR: photosynthetically
788 available radiation.

789 **Figure. 6.** BBSi and BDSi dynamics in the Severn Estuary in the summer (A) and
790 winter (B). Cylinders represent biofilm biomass. Dark arrows represent river sources.
791 Arrows represent export of BBSi (light grey) and BDSi (black) to the coastal zone.
792 BBSi: benthic biogenic silica. BDSi: benthic dissolved silicon.

Table Captions

793

794 **Table 1.** Notations for silicon parameters, nutrients, biomass and chlorophyll
795 fluorescence.

796 **Table 2.** Microphytobenthos biomass and variable chlorophyll fluorescence
797 parameters. Values reported with standard deviation ± *SD.* Chl *a*: chlorophyll *a*:
798 $n=36$(summer), $n=36$(winter). rETR$_{max}$: relative maximum Electron Transport Rate:
799 $n=34$(summer), $n=18$(winter). α: maximum light use coefficient: $n=34$(summer),
800 $n=18$(winter). F$_v$/F$_m$: ecological health, $n=34$(summer), $n=27$(winter). NPQ$_{max}$:
801 maximum non-photochemical quenching, $n=34$(summer), $n=17$(winter). F$_m'$: maximum
802 PSII Chl fluorescence yield in actinic light when all reaction centres are closed:
803 $n=34$(summer), $n=27$(winter). F$_m'm$: maximum F$_m'$ value under low actinic light,
804 $n=34$(summer), $n=17$(winter).

805 **Table 3.** Key drivers of BBSi and BDSi during the summer and winter in the Severn
806 Estuary. Pearson's correlations reported with coefficient values (*r*) and number of
807 samples (*n*). Significant correlations ($p<0.05$) are shown in **bold**. BBSi: benthic
808 biogenic silica. BDSi: benthic dissolved silicon. Chl *a*: chlorophyll *a.* rETR$_{max}$: relative

809   maximum Electron Transport Rate. α: maximum light use coefficient. F_v/F_m: ecological

810   health. NPQ: non-photochemical quenching.

A)

WALES

51°40'N

Central
Channel
North

51°30'N

Central
Channel
South

51°20'N

Inner Bristol Channel

51°10'N

ENGLAND

0   5   10   20 Miles

Newport Wetlands

Inner Severn
Estuary

Outer
Severn
Estuary

Severn Beach

Portishead

Tidal River
Severn

3°40'W   3°20'W   3°0'W   2°40'W   2°20'W

B)

C)

3°20'W   3°0'W   2°40'W

51°30'N

51°20'N

0 2.5 5   10 Miles

High : 13.4 m

Low : -34.9 m

D)

3°20'W   3°0'W   2°40'W

51°40'N

51°30'N

0 2.5 5   10 Miles

617 m

306 m

0
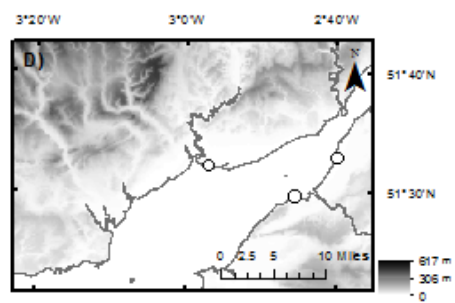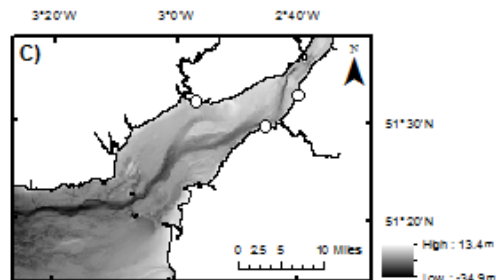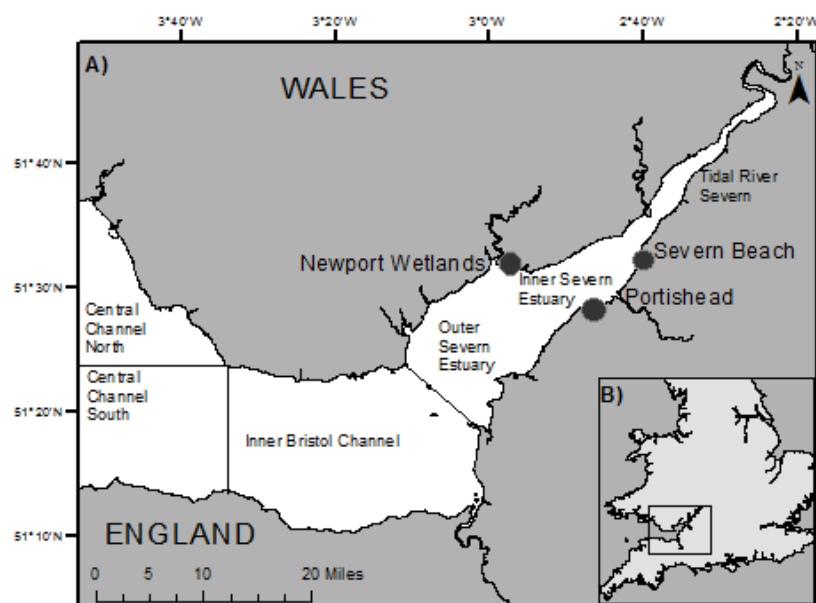
Parameter	Description
BSi	Biogenic silica
BBSi	Benthic biogenic silica
DSi	Dissolved silica
BDSi	Benthic dissolved silica
P	Orthophosphate
MPB	Microphytobenthos
Chl *a*	Chlorophyll *a* (proxy for biomass)
F'	Operational PSII Chl fluorescence yield in actinic light
F_m'	Maximum PSII Chl fluorescence yield in actinic light when all reaction centres are closed
$F_m'{}_{max}$	Maximum F_m'
RLC	Rapid Light Curve
PAR	Photosynthetically available radiation
$rETR_{max}$	Relative Maximum Electron Transport Rate
α	Maximum light use coefficient for PSII
F_q'/F_m'	Maximum quantum efficiency of PSII
F_v/F_m	Maximum photochemical yield (MPB biofilm health)
NPQ	Non-photochemical quenching
NPQ_{max}	Maximum non-photochemical quenching

A) Summer

Benthic dissolved silica (mg/L) — Benthic biogenic silica (%)

Upper inner estuary — Lower inner estuary

DSi / BSi

B) Winter

Benthic dissolved silica (mg/L) — Benthic biogenic silica (%)

Upper inner estuary — Lower inner estuary

DSi / BSi

C)

Orthophosphate (mg/L)

Upper inner estuary — Lower inner estuary

Summer / Winter

No P detected in summer

Severn Beach   Portishead   Newport Wetlands
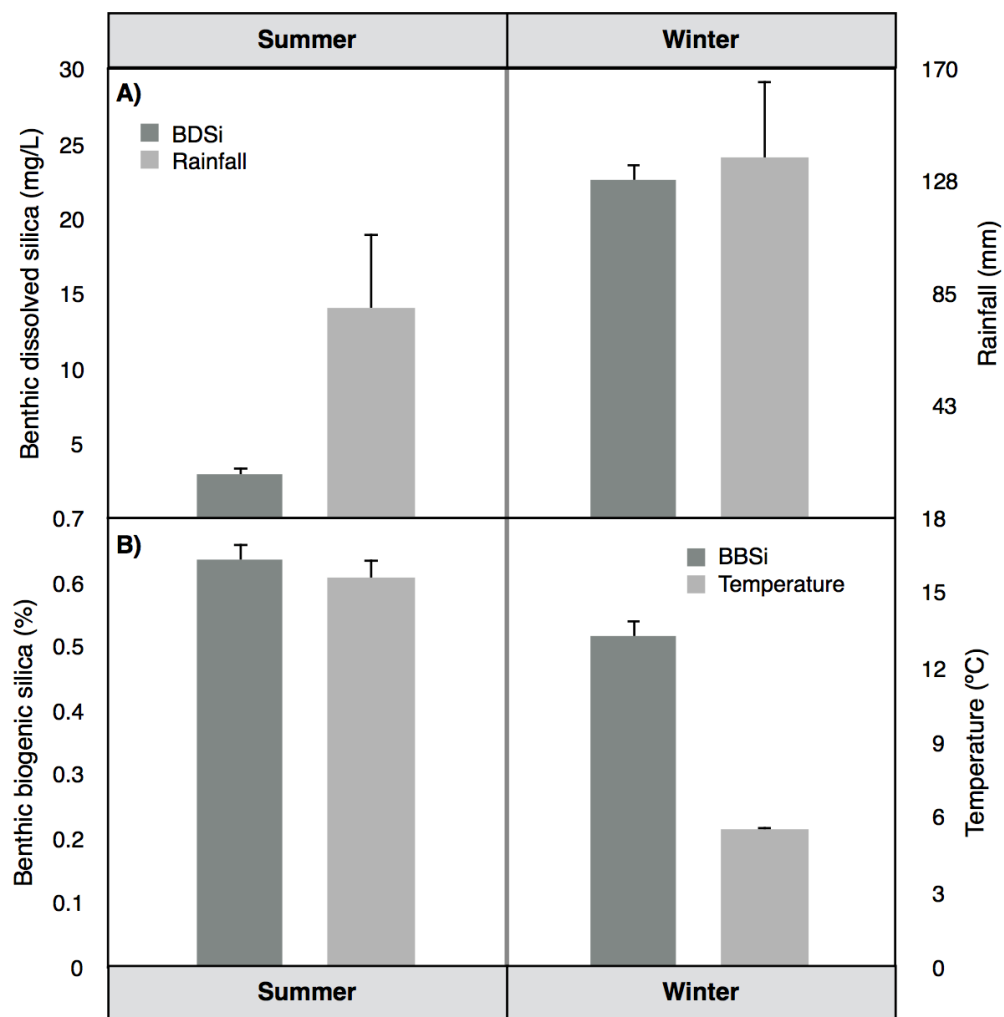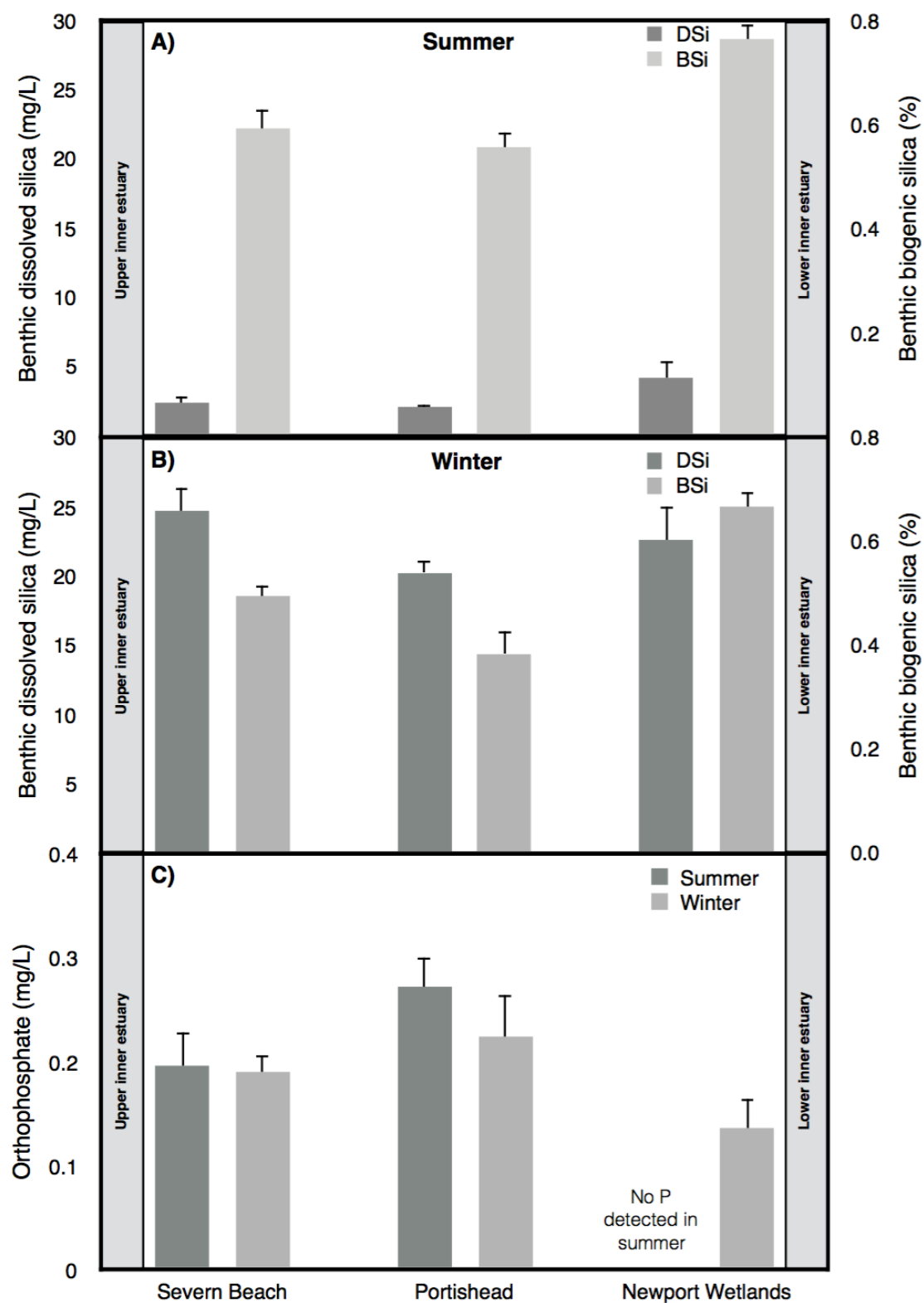
Location	Site	Chl a (mg g^{-1} sed. dw.)	Water content (%)	rETR$_{max}$ (rel. units)	α (µmol photons m^{-2} s^{-1})	F_v/F_m (rel. units)	NPQ$_{max}$ (rel. units)	$F_m'{}_{max}$ (rel. units)
Summer								
Severn Beach	1	11.0 ± 1.9	54.9 ± 0.4	257.2 ± 16.9	0.24 ± 0.02	0.48 ± 0.5	0.3 ± 0.03	1713 ± 180
Portishead	2	11.3 ± 2.1	51.8 ± 0.8	235.2 ± 27.6	0.23 ± 0.02	0.47 ± 0.0	0.12 ± 0.1	2314 ± 320
Newport Wetlands	3	17.3 ± 1.7	65.2 ± 0.6	269.8 ± 15.9	0.18 ± 0.03	0.36 ± 0.1	0.11 ± 0.1	1813 ± 332
Average		**13.2 ± 1.9**	**57.3 ± 0.6**	**254.1 ± 20.1**	**0.2 ± 0.02**	**0.44 ± 0.2**	**0.17 ± 0.1**	**1946 ± 277**
Winter								
Severn Beach	1	24.5 ± 2.6	53.2 ± 0.8	109.7 ± 21.5	0.10 ± 0.1	0.65 ± 0.1	0.17 ± 0.0	2765 ± 798
Portishead	2	21.3 ± 1.6	57.9 ± 0.8	97.3 ± 20.8	0.17 ± 0.04	0.63 ± 0.1	0.18 ± 0.0	3318 ± 637
Newport Wetlands	3	26.0 ± 2.8	53.8 ± 0.9	141.0 ± 39.1	0.20 ± 0.01	0.67 ± 0.0	1.3 ± 0.78	2601 ± 408
Average		**24.0 ± 2.3**	**55.0 ± 0.8**	**116.0 ± 27.1**	**0.16 ± 0.05**	**0.65 ± 0.1**	**0.84 ± 0.4**	**2894 ± 614**

Summer
Severn Beach   1   11.0 ± 1.9   54.9 ± 0.4   257.2 ± 16.9   0.24 ± 0.02   0.48 ± 0.5   0.3 ± 0.03   1713 ± 180
Portishead   2   11.3 ± 2.1   51.8 ± 0.8   235.2 ± 27.6   0.23 ± 0.02   0.47 ± 0.0   0.12 ± 0.1   2314 ± 320
Newport Wetlands   3   17.3 ± 1.7   65.2 ± 0.6   269.8 ± 15.9   0.18 ± 0.03   0.36 ± 0.1   0.11 ± 0.1   1813 ± 332

A) Summary
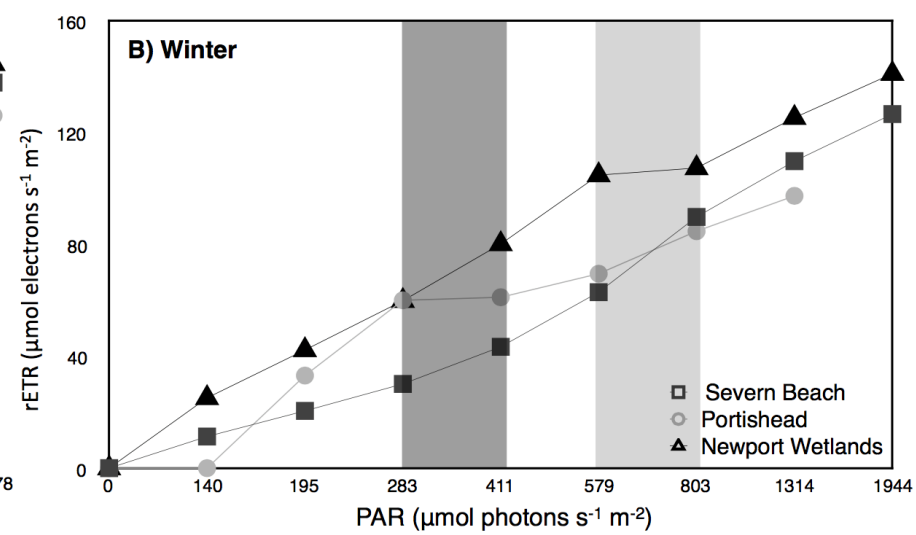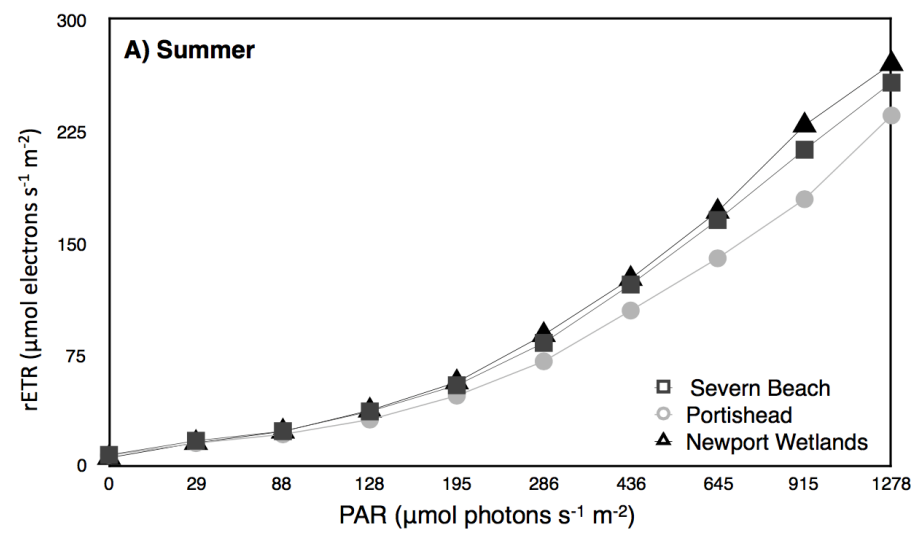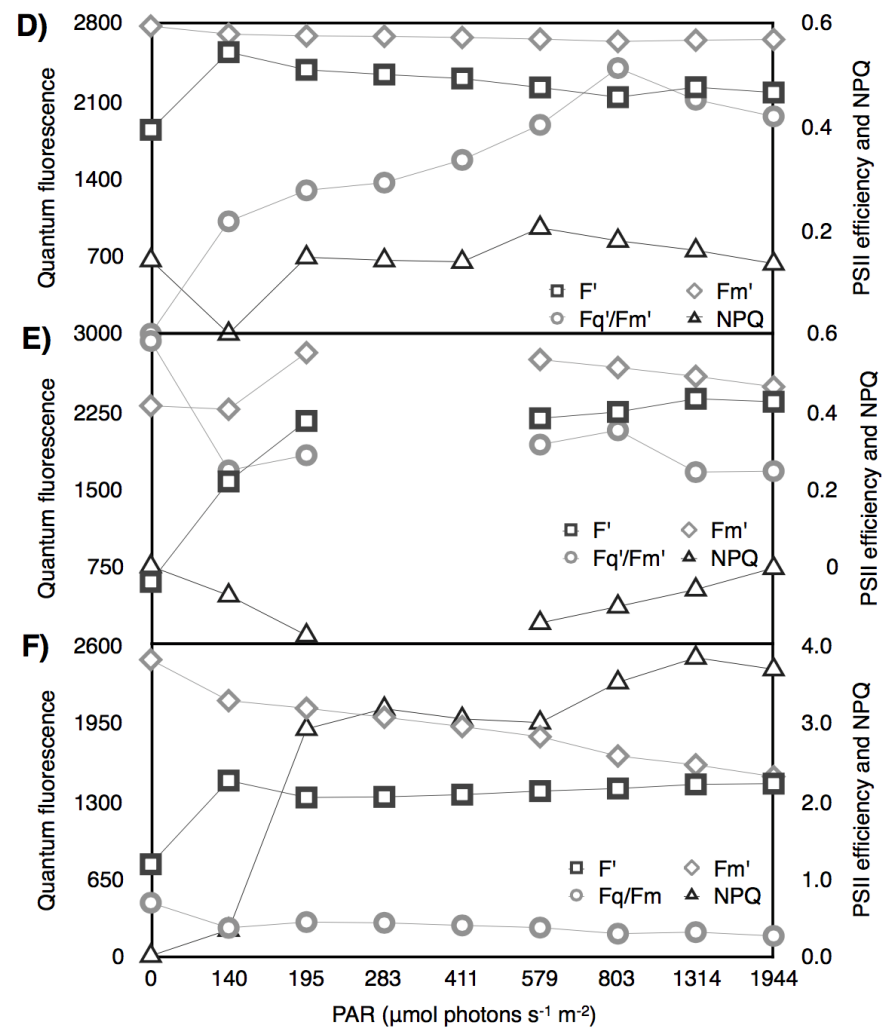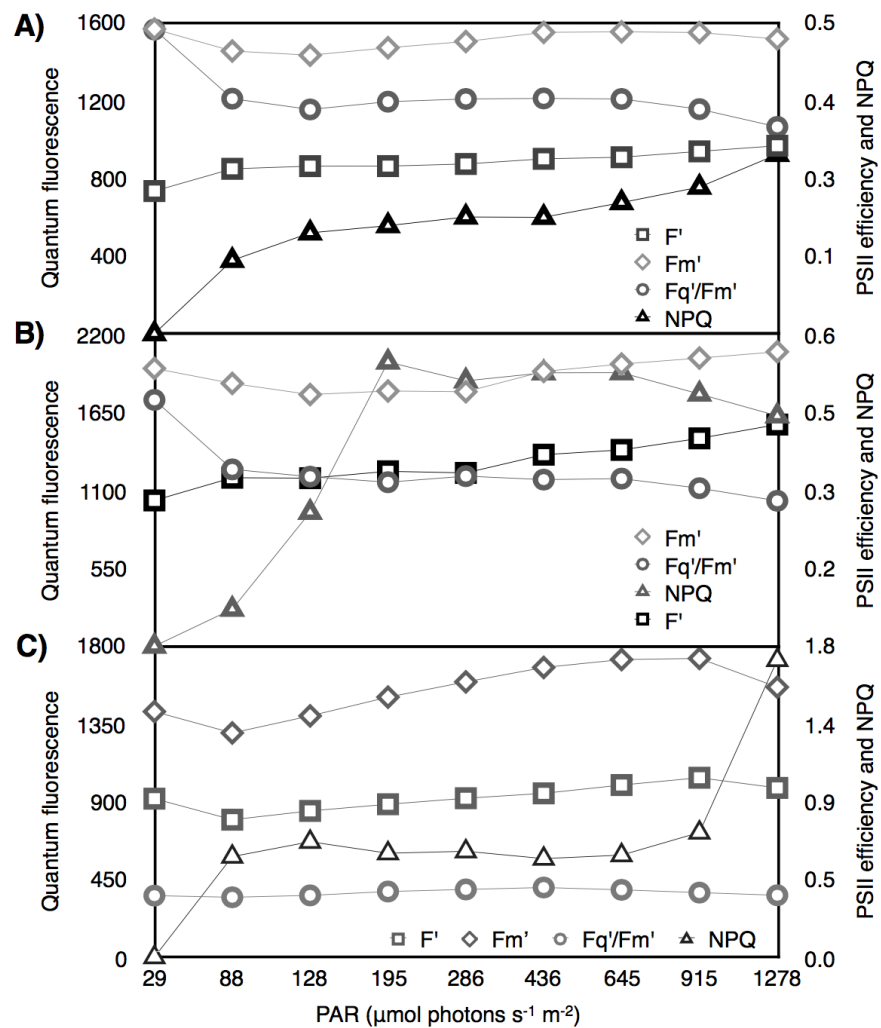
B) Winter

	Summer								Winter							
	Site 1		Site 2		Site 3		All		Site 1		Site 2		Site 3		All	
	n	r	n	r	n	r	n	r	n	r	n	r	n	r	n	r
BBSi drivers																
BDSi vs. BBSi	12	0.017	12	-0.242	12	-0.349	36	0.105	12	0.105	12	-0.048	12	0.271	36	0.168
P vs. BBSi	12	0.120	12	0.413	12	-	36	**-0.434**	12	-0.269	12	0.163	12	-0.256	36	0.223
Chl *a* vs. BBSi	12	-0.010	12	-0.049	12	0.226	36	**0.296**	12	0.411	12	**-0.607**	12	**0.541**	36	-0.264
rETR$_{max}$ vs. BBSi	11	**-0.679**	11	0.001	12	-0.471	34	-0.136	3	**0.877**	5	-0.410	10	**-0.617**	18	-0.058
α vs. BBSi	11	-0.259	11	0.380	12	-0.220	34	**-0.289**	3	-0.185	5	0.604	10	-0.411	18	0.203
F$_v$/F$_m$ vs. BBSi	11	-0.326	11	0.382	12	-0.224	35	**-0.291**	10	-0.058	5	-0.292	12	0.038	32	-0.001
NPQ vs. BBSi	11	**0.552**	11	0.127	12	**0.761**	34	**0.289**	3	-0.115	4	0.557	10	-0.0	17	0.226
BDSi drivers																
P vs. BDSi	12	0.160	12	0.444	12	-	36	-0.248	12	0.358	12	0.325	12	-0.485	36	-0.115
Chl *a* vs. BDSi	12	**0.498**	12	0.309	12	-0.239	36	0.160	12	-0.480	12	0.313	12	0.100	36	-0.022
rETR$_{max}$ vs. BDSi	11	0.132	11	-0.247	12	-0.018	34	0.069	3	-0.151	5	-0.011	10	-0.026	18	0.010
α vs. BDSi	11	-0.244	11	0.380	12	0.033	34	-0.160	3	**-0.987**	5	0.093	10	0.207	18	-0.040
F$_v$/F$_m$ vs. BDSi	11	-0.215	11	-0.409	12	0.061	35	-0.135	10	0.205	5	-0.211	12	0.209	32	0.147
NPQ vs. BDSi	11	0.018	11	0.044	12	-0.082	34	-0.053	3	**-0.972**	4	0.193	10	-0.328	17	-0.286

A) Summer

River Wye

River Severn

DSi = ?
BSi = ?

Newport Wetlands
BBSi = 0.8%
BDSi = 4.2±1.2 mg L^{-1}

River Usk

Mineralization

Deposited Si

Severn Beach
BBSi = 0.6%
BDSi = 2.3 ± 0.5 mg L^{-1}

Export of Si to coastal zone

BBSi = 0.6%

River Avon

BDSi = 2.9 ± 0.5 mg L^{-1}

Portishead
BBSi = 0.6%
BDSi = 2.1± 0.1 mg L^{-1}

N

10 miles

B) Winter

River Wye

River Severn

DSi = ?
BSi = ?

Newport Wetlands
BBSi = 0.7%
BDSi = 22.1±2.4 mg L^{-1}

River Usk

Mineralization

Deposited Si

Severn Beach
BBSi = 0.5%
BDSi = 24.7±1.6 mg L^{-1}

Export of Si to coastal zone

BBSi = 0.5%

River Avon

BDSi = 22.5±1.0 mg L^{-1}

Portishead
BBSi = 0.4%
BDSi = 20.3 ± 0.9 mg L^{-1}

N

10 miles